uum flux ratio that we observed is an order of magnitude greater than that in the core [$F_{\rm line}/F_{\rm continuum}$ is ~1 for our east jet but is ~0.1 for the 7.3-keV line in Chandra HETGS observations (*6*)]. The lines from these extended jets are still an order of magnitude weaker than the moving core x-ray lines (*5, 6*) and would not be expected to show measurable changes in their Doppler shifts (unless, e.g., a major outburst from SS 433 resulted in enhanced emission at some particular precession phase). Nevertheless, they should be present as weak features in spectra that do not spatially resolve the core and jets.

Reheating (in situ acceleration) of a leptonic (electron and possibly also positron) component of jet plasma, presumably by conversion of the jet kinetic energy, is commonly invoked to explain synchrotron or inverse Compton energy emission on large scales in the jets of AGN (*15–17*). The reheating of the baryonic plasma that we observed in SS 433 requires a similar tapping of the bulk kinetic energy of the flow, by processes that are able to act on atomic nuclei. In the internal shock model for blazars (*16*), a slightly varying jet speed results in shocks downstream in the jet flow. In the context of this model, random discrepancies of ~15% in the velocity of the jets from SS 433, inferred from long-term optical monitoring (*3*), could produce shocks a few hundred days downstream (for a precession period of 162 days and a mean jet velocity of 0.26*c*), comparable to what we observed (*18*).

To conclude, these observations spatially resolve a line-emitting region in a relativistic jet. They reveal that the hot x-ray–emitting region is still moving relativistically on physical scales that are orders of magnitude larger than previously inferred, with no evidence for substantial deceleration, supporting models for extended x-ray jets in AGN that require bulk relativistic motion on large physical scales (*15*). Furthermore, this observation demonstrates that particle reacceleration in a relativistic jet, previously inferred only to act on the leptonic component, can act also on atomic nuclei. Comparison of this highly super-Eddington, mass-loaded jet with those of other x-ray binary systems and AGN can provide unique insights into the matter and energy content of relativistic jets and hence the coupling of accretion and outflow in conditions of extreme gravity, pressure, and energy density.

References and Notes

1. G. O. Abell, B. Margon, *Nature* **279**, 701 (1979).
2. R. M. Hjellming, K. J. Johnston, *Nature* **290**, 100 (1981).
3. S. S. Eikenberry *et al.*, *Astrophys. J.* **561**, 1027 (2001).
4. W. Brinkmann, N. Kawai, M. Matsuoka, H. H. Fink, *Astron. Astrophys.* **241**, 112 (1991).
5. T. Kotani, N. Kawai, M. Matsuoka, W. Brinkmann, *Publ. Astron. Soc. Pac.* **48**, 619 (1996).
6. H. L. Marshall, C. R. Canizares, N. S. Schulz, *Astrophys. J.* **564**, 941 (2002).
7. J. Shaham, *Vistas Astron.* **25**, 217 (1981).
8. W. Brinkmann, B. Aschenbach, N. Kawai, *Astron. Astrophys.* **312**, 306 (1996).
9. G. M. Dubner, M. Holdaway, W. M. Goss, I. F. Mirabel, *Astron. J.* **116**, 1842 (1998).
10. Pileup is an effect by which two or more photons that hit the same pixel on the CCD in one integration are counted as a single photon. If the summed energy is greater than the ACIS threshold (~15 keV), the detection is rejected, and no counts are recorded.
11. J. F. Dolan *et al.*, *Astrophys. J.* **327**, 648 (1997).
12. The orbital phase $0 \leq \phi \leq 1$ indicates the fraction of one entire orbit completed. Eclipse of the x-ray source (i.e., superior conjunction of the neutron star or black hole) corresponds to $\phi = 0$. The orbital period is 13.08 days.
13. The precession phase $0 \leq \psi \leq 1$ indicates the fraction of one entire jet precession cycle. $\psi = 0$ is, by convention (*2*), one of the two instances when the beams of SS 433 are perpendicular to the line of sight. The precessional period is 162.4 days.
14. The Doppler factor $\delta = [\gamma(1 - \beta \cos \theta)]^{-1}$ where velocity $v = \beta c$, c is the speed of light, $\gamma = (1 - \beta^2)^{-1/2}$ is the Lorentz factor, and θ is the angle to the line of sight.
15. D. E. Harris, H. Krawczynski, *Astrophys. J.* **565**, 244 (2002).
16. M. Spada, G. Ghisellini, D. Lazzati, A. Celotti, *Mon. Not. R. Astron. Soc.* **325**, 1559 (2001).
17. G. V. Bicknell, D. B. Melrose, *Astrophys. J.* **262**, 511 (1982).
18. The relation $\Delta t = P(1 - \delta)/2\delta$, where P is the precession period and δ is the fractional deviation from the mean velocity v_m of the ejected blobs, gives the time interval Δt over which a blob with velocity $(1 + \delta)v_m$ reaches the blob launched with velocity $(1 - \delta)v_m$ at the same precessional phase one cycle earlier. Using $P = 162$ days and $\delta = 0.15$, we obtain $t \sim 450$ days.
19. The top panel of Fig. 1 is reproduced from figure 1 in (*9*) by permission of the American Astronomical Society.
20. We thank D. Harris and M. van der Klis for comments on a draft of this manuscript and W. Brinkmann and M. Watson for earlier useful discussions. M.M. and R.F. are grateful to staff members at the Max-Planck-Institut für Astrophysik for their hospitality during the initial analysis of these data.

6 May 2002; accepted 30 July 2002

Internal Olefins to Linear Amines

A. Seayad, M. Ahmed, H. Klein, R. Jackstell, T. Gross, M. Beller*

The selective synthesis of linear amines from internal olefins or olefin mixtures was achieved through a catalytic one-pot reaction consisting of an initial olefin isomerization followed by hydroformylation and reductive amination. Key to the success is the use of specially designed phosphine ligands in the presence of rhodium catalysts. This reaction constitutes an economically attractive and environmentally favorable synthesis of linear aliphatic amines.

Linear aliphatic amines are used for the production of solvents, fine chemicals, agrochemicals, pharmaceutical intermediates, and vulcanization accelerators. They are also sold as catalysts for the production of polymers, especially polyurethanes. Fatty amines are useful as fabric softeners, corrosion inhibitors, and emulsifiers as well as in ore flotation. Important industrial methods for their synthesis include reductive amination of the corresponding aldehydes and hydrogenation of the respective nitriles, which are both available from terminal olefins (*1*). In addition, a number of less atom-efficient methods—such as classical nucleophilic substitution reactions of alkyl halides, or less general methods like hydroamination of olefins—have been developed on laboratory scales (*2*). Thus, there is considerable interest in developing versatile and direct preparation routes to amines using economically more attractive feedstock.

Because of the importance of linear amines and alcohols, the *anti*-Markovnikov reaction of terminal olefins with N- or O-nucleophiles (where the nucleophile adds selectively to the terminal position of the olefin) is an important goal for catalysis. Despite some progress (*1–3*), no general methodology for such reactions has been achieved so far with aliphatic olefins. Even more challenging is the synthesis of the linear functionalized products from internal olefins. Such a process would be of value to the chemical industry, because mixtures of internal aliphatic olefins, such as butenes, hexenes, and octenes, are substantially cheaper and more easily available than the pure terminal isomers. Hence, in recent years special interest has been paid to hydroformylation reactions of internal olefins to give linear aldehydes (*4–7*).

An environmentally benign (atom-efficient, one-pot) synthesis of amines from olefins is the so-called hydroaminomethylation reaction (*8*). This domino reaction consists of initial hydroformylation of the olefin to an aldehyde and subsequent formation of an enamine (or imine) followed by hydrogenation. Since its discovery by Reppe at BASF, the hydroaminomethylation reaction has been mainly studied in industry. More recently, Eilbracht and co-workers developed new methodologies based on tandem sequences using the hydroaminomethylation reaction (*8*).

To produce linear amines from internal

Institut für Organische Katalyseforschung an der Universität Rostock e.V. (IfOK), Buchbinderstrasse 5-6, D-18055 Rostock, Germany.

*To whom correspondence should be addressed. E-mail: matthias.beller@ifok.uni-rostock.de

olefins via hydroaminomethylation, a suitable catalyst must fulfill a number of requirements. It must catalyze fast isomerization between the internal and terminal olefins (Fig. 1, reaction a). Because the thermodynamic equilibrium mixture contains, in general, <5% of the terminal olefin, the hydroformylation of the terminal olefin (Fig. 1, reaction c) must occur faster and with high *n*-selectivity compared to the reaction of the internal olefin (Fig. 1, reaction b). Finally, the catalyst must be active and selective for enamine (or imine) hydrogenation (Fig. 1, reaction d).

No hydroaminomethylation reaction of internal olefins has been reported that gives the linear products. The main problem of this reaction is the low isomerization activity of the corresponding rhodium catalyst in the presence of strong σ-donor ligands (e.g., amines). Although hydridorhodiumcarbonyl species are active olefin isomerization catalysts, this reaction is normally prevented by the addition of basic phosphines or amines (*9*). Hence, no isomerization of internal olefins in hydroformylations in the presence of amines leading to the linear product appears to have been reported. We sought to realize the selective hydroaminomethylation of internal olefins by using derivatives of 2,2′-bis-(diphenylphosphinomethyl)-1,1′-binaphthyl [NAPHOS (*10*, *11*)], which we have recently developed for rhodium-catalyzed hydroformylation reactions of internal olefins (*7*).

Because butenes are the most important industrial mixture of internal and terminal olefins [more than 25 billion kg per year are produced (*12*)], investigations were carried out mainly with *E*/*Z*-2-butene as the raw material. Optimization studies showed that excellent yields and selectivity to the linear amine can be achieved at 120°C and 40 to 60 bar CO/H_2 (1:3 to 1:5) in toluene/tetrahydrofuran mixture (1:1) as a solvent system.

For comparison, well-known mono- and bidentate phosphines and phosphites were tested. None of these ligands gave considerable amounts of the linear amine. Phosphite ligands are less suitable for the desired reaction because of hydrolysis problems encountered in the presence of water and amines. Therefore, we focused our attention mainly on phosphine ligands, which can isomerize internal olefins in the presence of CO. So far, only two classes of phosphine ligands [NAPHOS and XANTPHOS (*13*) systems] are reported that can effect this reaction. Unfortunately, NAPHOS gave only 6% of the linear amine. The formation of linear enamines in moderate selectivity indicates its initial isomerization and hydroformylation activities, but the low yield of amine shows the inefficient hydrogenation of the enamines with NAPHOS as a ligand. As shown in Table 1, all tested NAPHOS-like ligands performed poorly in the hydrogenation step except for 2,2′-bis[di(3,5-trifluoromethylphenyl)phosphinomethyl]-1,1′-binaphthyl (IPHOS), which gave *n*-pentylpiperidine in high yield (88%) (*14*). The considerable difference between IPHOS and other NAPHOS derivatives is especially noteworthy. Small differences in the steric and electronic nature of the aryl group have a substantial—and so far unpredictable—effect on selectivity and activity.

A lower reaction temperature (100°C) favored the formation of the linear product [linear to branched product ratio (l:b) = 96:4] (Table 2). However, to obtain sufficient hydrogenation of the enamine, it is desirable to attain a reaction temperature of 120°C. Even at this temperature, no ligand degradation was seen in ^{31}P nuclear magnetic resonance after >20 hours, which demonstrates the stability and potential use of the ligand. In addition to the reaction temperature, the partial pressure of H_2 and CO and the concentrations of amine and olefin influence the selectivity of the reaction.

Apart from the reaction of 2-butene and piperidine, other internal olefins (2-pentene, 2-hexene, 2-octene, 3-hexene) and amines (dimethylamine, di-*n*-hexylamine, *n*-hexylamine) also reacted well in the presence of 0.1 mol % $[Rh(cod)_2]BF_4$ and 0.4 mol % IPHOS, giving preferentially the correspond-

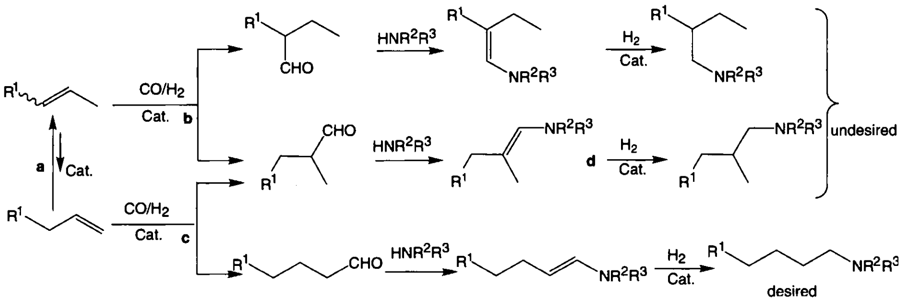

Fig. 1. Selective hydroaminomethylation of internal olefins (R^1 = alkyl; R^2, R^3 = H, alkyl).

Table 1. Hydroaminomethylation of 2-butene: ligand effect (*18*). Reaction conditions: $[Rh(cod)_2BF_4]$, 0.1 mol %; ligand:Rh ratio, 4:1; toluene, 15 ml; THF, 15 ml; P_{CO}, 10 bar; P_{H2}, 50 bar; piperidine, 15.0 mmol; temperature, 120°C; time, 24 hours.

2-Butene: piperidine	Ligand	Conversion (%)	Total amine selectivity (%)	Linear amine selectivity (%)	l:b
1.3:1	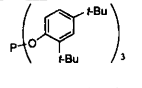	91	10	0	<0:100*
1.3:1	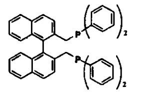	50	6	6	>99:1*
1.1:1	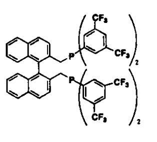	100	97	88	90:10
1.5:1	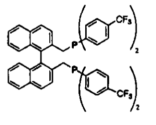	100	11	11	>99:1*

*Major side products are linear and branched enamines.

Table 2. Hydroaminomethylation of 2-butene in the presence of IPHOS (*17*). Reaction conditions: $[Rh(cod)_2BF_4]$, 0.1 mol %; piperidine, 15.0 mmol; Rh:IPHOS ratio, 1:4; toluene, 15 ml; THF, 15 ml; P_{CO}, 10 bar; P_{H2}, 50 bar; time, 24 hours except where indicated.

2-Butene/ piperidine	Temp. (°C)	Conversion (%)	Total amine selectivity (%)	Linear amine selectivity (%)	l:b	TON
1:1	100	100	54	52	96:4	540
1.1:1	120	100	97	88	90:10	970
1.1:1	140	100	98	78	78:22	980*
2:1	120	100	91	87	96:4	910

*Time, 12 hours.

Table 3. Hydroaminomethylation of different olefins. Reaction conditions: olefin, 15 mmol; amine, 15 mmol; $[Rh(cod)_2]BF_4$, 0.1 mol %; IPHOS, 0.4 mol %; toluene, 15 ml; THF, 15 ml; P_{CO}, 10 bar; P_{H_2}, 50 bar; temperature, 120°C; time, 24 hours.

Olefin	Amine	Conversion (%)	Total amine selectivity (%)	Linear amine selectivity (%)	l:b	TON
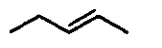		88	98	82	82:18	862
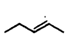	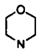	71	69	53	72:28	490
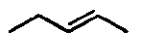	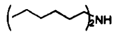	78	90	83	91:9	702
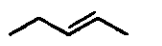		100	65	74	78:22	650
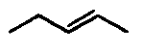	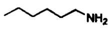	80	87	62	71:29	696
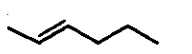		77	91	76	78:22	701
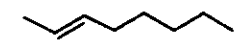		60	96	90	94:6	576
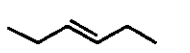	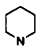	88	96	68	71:29	563*

*3-Hexene, 10 mmol; piperidine, 10 mmol.

ing linear amines in good to excellent yields (Table 3). The reaction of 2-pentene and piperidine also proceeded smoothly in the presence of 0.05 mol % Rh [turnover number (TON) ≈ 2000]. However, a reaction time of 48 hours was needed to achieve complete conversion.

The reaction of the primary amine (*n*-hexylamine) occurs with high regio- and chemoselectivity, despite the further potential amination to yield tertiary amines. This reaction constitutes one of the rare examples of a hydroaminomethylation reaction of a primary amine to selectively give the secondary amine. In addition, 3-hexene, 3-octene, etc., also provide the corresponding linear amines preferentially under the present reaction conditions.

In general, the reaction sequences reported proceed with 90 to 95% atom efficiency and leave only water as the byproduct. Although the catalyst productivity (TON = 2000) has already been developed to a useful level, further improvements should be possible.

References and Notes

1. A. Ricci, Ed., *Modern Amination Methods* (Wiley-VCH, Weinheim, Germany, 2000).
2. T. E. Müller, M. Beller, *Chem. Rev.* **98**, 675 (1998).
3. For a recent review, see (*15*).
4. L. A. van der Veen, P. C. J. Kamer, P. W. N. M. van Leeuwen, *Angew. Chem. Int. Ed.* **38**, 336 (1999).
5. D. Selent, K.-D. Wiese, D. Röttger, A. Börner, *Angew. Chem. Int. Ed.* **39**, 1639 (2000).
6. For a general review of hydroformylation of both internal and terminal olefins, as well as the ligand effects, see (*16*).
7. H. Klein, R. Jackstell, K.-D. Wiese, D. Röttger, M. Beller, *Angew. Chem. Int. Ed.* **40**, 3408 (2001).
8. For a general review of hydroaminomethylation reactions, see (*17*).
9. M. E. Broussard *et al.*, *Science* **260**, 1784 (1993).
10. K. Tamao *et al.*, *Tetrahedron Lett.* **16**, 1389 (1977).
11. W. A. Hermann, R. Schmid, C. W. Kohlpaintner, T. Priermeier, *Organometallics* **14**, 1961 (1995).
12. K. Weissermel, H.-J. Arpe, *Industrielle Organische Chemie* (Wiley-VCH, Weinheim, Germany, ed. 5, 2000).
13. P. W. N. M. van Leeuwen, P. C. Kamer, J. N. H. Reek, P. Dierkes, *Chem. Rev.* **100**, 2741 (2000).
14. All hydroaminomethylation experiments were carried out in a Parr stainless steel autoclave (100 ml). In a typical experiment, the autoclave was charged with $[Rh(cod)_2]BF_4$ (0.1 mol %), IPHOS (0.4 mol %), piperidine (15 mmol), tetrahydrofuran (15 ml), and toluene (15 ml) under argon atmosphere. The autoclave was cooled with freezing mixture after closing, and 2-butene (15 to 16 mmol) was condensed into it. The autoclave was pressurized with CO (10 bar) and hydrogen (50 bar) and the reaction was carried out at 120°C for 24 hours. After reaction, the autoclave was cooled to 0° to 5°C and then depressurized, and the contents were transferred to a Schlenk flask under argon atmosphere, dried over $MgSO_4$, and analyzed by gas chromatography [HP-5890 series; column, HP5 (crosslinked 5% PH ME Siloxane), 30 m by 0.25 mm] using bis(methoxyethyl)ether as an internal standard.
15. M. Beller *et al.*, *Synlett*, in press.
16. P. W. N. M. van Leeuwen, C. Claver, Eds., *Rhodium Catalyzed Hydroformylation* (Kluwer Academic, Dordrecht, Netherlands, 2000).
17. P. Eilbracht *et al.*, *Chem. Rev.* **99**, 3329 (1999).
18. Additional examples are given in expanded tables at *Science* Online.
19. We thank A. Tillack for general discussions. Supported by a fellowship from the Alexander-von-Humboldt-Stiftung (A.S.) and by the state Mecklenburg-Vorpommern, Fonds der Chemischen Industrie, and Bundesministerium für Bildung und Forschung.

Supporting Online Material
www.sciencemag.org/cgi/content/full/297/5587/1676/DC1
Materials and Methods
Tables S1 and S2

7 June 2002; accepted 23 July 2002

Lead Isotopic Ages of Chondrules and Calcium-Aluminum–Rich Inclusions

Yuri Amelin,[1]*† Alexander N. Krot,[2] Ian D. Hutcheon,[3] Alexander A. Ulyanov[4]

The lead-lead isochron age of chondrules in the CR chondrite Acfer 059 is 4564.7 ± 0.6 million years ago (Ma), whereas the lead isotopic age of calcium-aluminum–rich inclusions (CAIs) in the CV chondrite Efremovka is 4567.2 ± 0.6 Ma. This gives an interval of 2.5 ± 1.2 million years (My) between formation of the CV CAIs and the CR chondrules and indicates that CAI- and chondrule-forming events lasted for at least 1.3 My. This time interval is consistent with a 2- to 3-My age difference between CR CAIs and chondrules inferred from the differences in their initial $^{26}Al/^{27}Al$ ratios and supports the chronological significance of the ^{26}Al-^{26}Mg systematics.

Chondritic meteorites (chondrites) consist of three major components: refractory CAIs, less refractory ferromagnesian silicate spherules called chondrules, and a fine-grained matrix. It is generally believed that CAIs and chondrules formed in the solar nebula (a disk of dust and gas surrounding the proto-Sun) by high-temperature processes that included condensation, evaporation, and, for all chondrules and many CAIs, subsequent melting during multiple brief heating episodes (*1–3*). The mechanisms involved in chondrule formation are uncertain: shock waves, lightning discharges, and X-wind (jet flow) are currently being considered (*2*, *4–8*). The existing estimates for the timing of CAI and chondrule formation are either controversial or insufficiently precise. Thus, the total duration of CAI and chondrule formation,

---

[1] Department of Earth Sciences, Royal Ontario Museum, Toronto, ON M5S 2C6, Canada. [2] Hawaii Institute of Geophysics and Planetology, School of Ocean and Earth Science and Technology, University of Hawaii, Honolulu, HI 96822, USA. [3] Lawrence Livermore National Laboratory, Livermore, CA 94451, USA. [4] M. V. Lomonosov Moscow State University, Moscow 117999, Russia.

*Present address: Geological Survey of Canada, 601 Booth Street, Ottawa, ON K1A 0E8, Canada.

†To whom correspondence should be addressed. E-mail: yamelin@NRCan.gc.ca